Photovoltaic cells based on lead- and tin-perovskites

Ricardo Carvalho

Abstract

This work is focused on the fabrication and characterization of lead- and tin-perovskite photovoltaic cells. More than one hundred cells with different perovskite solutions and different electron acceptor and hole transport layers, were produced and tested, aiming at obtaining the highest power conversion efficiency (PCE).

The best result was obtained for a solar cell based on methyl ammonium lead iodide, with a short-circuit current of 4.09 mA.cm^{-2}, an open circuit voltage of 0.57 V, a fill factor of 37.82% and PCE of 0.88%.

Despite the large number of fabrication conditions and perovskite compositions tested, the obtained results fail far below the reported performances. This points to the key role played by the preparation details, a knowledge that the hosting group has started to gather with this project.

Keywords: Perovskite, photovoltaic solar cells, methyl ammonium iodide, tin iodide, lead iodide, lead chloride.

1. Introduction

We face the conjecture of living in a society increasingly industrialized and globalized which focuses its efforts on growing technological empowerment [1].

Solar energy stands out for its high application potential as a renewable source among the many alternative energy sources. The sun is the world's most abundant energy resource providing approximately 5.4 x 10^{26} J of energy per year on Earth [2].

Solar energy is being captured in thermal systems and is used to generate, solar fuels in which hydrogen is included.

This photonic energy can also be used to generate, directly, electric energy, via the use of photovoltaic cells (where they can capture energy from the sun (photons) over a limited energy or wavelength range of radiation and convert light into electrical energy). The decade of 1980s marks the debut of the growing usage of these energetic systems. Their applications were initially confined to campers and boats, temporary power needs for some disaster situations or for remote communication stations repeaters [3].

Ten years later, the photovoltaic energy began to be widely used as an energy source for urban centers, private homes and office buildings becoming extremely important for the development of the modern world [3].

This technology has already gained a significant share among the various electric energy sources being used not only on Earth but also in Space applications.

Though silicon is the dominant semiconductor used to fabricate photovoltaic cells, other materials have been investigated over the years. Since 2009, perovskites have gained a special place among the new materials, showing a very fast rise in power conversion efficiency. These materials share the same crystalline structure as the calcium titanium oxide (CaTiO$_3$) mineral discovered in Ural Mountains (Russia) by the mineralogist L.A. Perovsk. Perovskites are much less expensive than silicon, can be processed from solution and nowadays they can offer an efficiency that rivals that of the crystalline silicon-based devices.

Perovskites have the general composition ABX$_3$, where X can be oxygen, carbon, nitrogen or halogen, A represents the larger cation that occupies octahedral cube-area coordinated by twelve X anions; and B is the smaller cation, which is stabilized in the octahedral region and coordinated by six X anions [4].

The active layer of photovoltaic solar cells is made of semiconductors. This has the key

role of absorbing the photons, generating free charges.

Inorganic semiconductors have an energy diagram composed by a valence band (VB) and a conduction band (CB). Normally, the excitation of electrons from the valence band (VB) to the conduction band (CB) is promoted by temperature. In other cases, this excitation can be promoted by photon absorption. For this photoexcitation to occur it is necessary that the photon energy is equal to or higher than the semiconductor band gap [5].The electron excitation is accompanied by the creation of hole (positive charge) in the VB. After this excitation, excited electrons and holes can be separated or recombined. The energy associated to the return of the electron to the VB can be re-emitted, a process named luminescence, or can be converted into heat. These basic principles, make semiconductors the required photoactive materials in photovoltaic applications [5].

In inorganic solar cells, a p-n junction is used to separate the excited electron (in the conduction band (CB)) from the hole (left in the valence band (VB)), before they recombine. Should this happen, the excited electron returns to the VB, annihilating the hole, and the energy is released as heat or as re-emitted light.

Organic semiconductors have a similar energy diagram: there is an energy gap between occupied bonding π orbitals (the HOMO designating the highest occupied molecular orbital) and empty anti-bonding π orbitals (the LUMO designating the lowest unoccupied molecular orbital). The excitation principle is quite the same as in the inorganic semiconductors. When a photon with equal or higher energy of the semiconductor gap is absorbed by the active layer it will excite an electron, generating a pair of positive and negative polarons, which, at variance with the inorganic semiconductors, have a significant binding energy, and that is named exciton. To split the exciton, and generate charges (polarons) we make use of heterojunctions: interfacing two materials with a LUMO energy mismatch above ca. 0.3 eV (typically 0.5 eV) to overcome the exciton binding energy. The material with higher LUMO is named electron-donor, being the other the electron acceptor. After photo-generation, excitons

have to diffuse to that heterojunction, before they recombine, to be splitted.

The main parameters used to characterize solar cells are: short-circuit current, J_{sc} which represents the current without any external applied voltage; open circuit voltage, V_{oc} which is the minimum voltage that we need to apply to the solar cell to nullify J_{sc}; fill factor, FF (Equation.1) which can be defined as the deviation from a squared J(v) "curve" (ideal cell); and power conversion efficiency, PCE (Equation.2) which is the efficiency of the cell.

$$FF = \frac{(Jm * Vm)Max}{Jsc * Voc} \tag{1}$$

$$\eta = \frac{Pm}{E * Ac} = \frac{Jsc * Voc * FF}{Pin} \tag{2}$$

The above parameters are calculated from the current-voltage curve of the solar cell recorded under illumination, typically from a solar simulator at 1 Sun (100mW/cm^2). The same curve is usually recorded in the dark to access the diode behavior of the cell. The typical J-V curves are showed in figure 1-1.
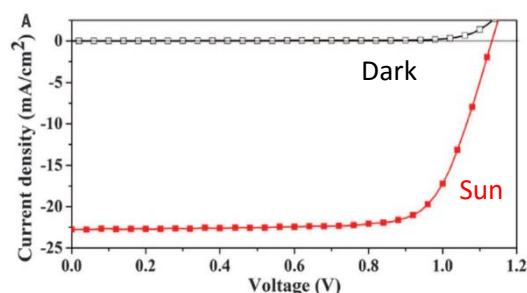

Figure 1-1.Typical J-V curve of solar cell in the dark and under illumination. Adapted from [6]

2. Experimental

During this work were produced approximately one hundred devices, all of them with planar structures. Each solar cell was composed by glass substrate, bottom electrode, hole-transporting material (HTM), perovskite layer, electron-accepting layer (EAL) and top electrode. The bottom contact

of solar cells consists on a thin layer of (ITO) indium-tin oxide. This degenerate n-type semiconductor with an optical band gap of approximately 3.7 eV behaves as transparent in the visible spectral region, but almost opaque in the UV and Infra-red regions [6] which make this semiconductor a good option to be used as a transparent conducting oxide (TCO) [7]. All glass substrates measured 1.2 x 1.2 cm^2 and contained a central ITO stripe 8 mm wide. Prior to the deposition of the hole-transporting material (HTM), the substrates surface was treated with oxygen plasma in order to obtain a hydrophilic surface and then, to promote better spreading and adhesion of HTM material (PEDOT: PSS) over the glass/ITO surface.

To create the hole-transporting layer, two different materials were tested; PEDOT: PSS and molybdenum oxide (MoO_3). PEDOT: PSS is a blend of the conjugated polymer poly (3,4-ethylenedioxythiophene) and of the doping polymer poly (styrenesulfonic acid) [8]. The PEDOT part carries the positive charges while PSS (composed by deprotonated sulfonyl groups) contains the negative charges. PEDOT: PSS has a work function of 5.2 eV producing an efficient hole collection [9]. This material was deposited from a water dispersion (from Heraeus) by spin coating and annealed during 10 min. MoO_3 (molybdenum oxide) is a stable phase transition metal oxide in which the most stable oxidation state of Mo is +6. It is much less toxic when compared with other heavy metals used in photovoltaic cells. This material can be a great alternative over the PEDOT: PSS layer because of their relatively high work function (5.3 - 5.7 eV) and its semi conductive properties due to hyper-stoichiometry produced by oxygen vacancies [10]. This material was deposited by PVD – thermal evaporation.

The electron-donor layer is composed by perovskite film. During this work four different perovskite systems were studied: methyl ammonium tin-iodide ($CH_3NH_3SnI_3$); methyl ammonium tin iodide-bromide ($CH_3NH_3SnIBr_2$); cesium tin iodide with tin fluoride ($CsSnI_3+SnF_2$); methyl ammonium lead iodide ($CH_3NH_3PbI_3$). For each one of these systems, different deposition and annealing conditions were tested, trying to obtain a smooth perovskite film surface. An alternative electron-donor material, a conjugated polymer named F8T2Ox1 was also tested. The perovskite solutions were prepared and deposited inside a nitrogen-filled glovebox.

i. Four different MAI:PbI_2 molar ratios were studied. The first set of "solutions" was prepared with a 1:1 molar ratio following several reports. We could not obtain clear solutions. For this reason, we tried different molar ratios, as an excess of MAI assists the PbI_2 dissolution. Therefore, MAI:PbI_2 molar ratios of 5:1, 1.5:1 and 1.28:1 were used, trying to minimize the excess of MAI while retaining the solubility. All solutes were dissolved in DMF in order to obtain a concentration of 30 – 40 wt% and were left stirring 12h at various temperatures in the range of 60 - 120 ºC. The precursor solution was then deposited by spin coating at different spinning speeds during different times and then submitted to different annealing conditions. A novel mixture with MAPbI$_3$ and small amounts of Polyethylene oxide (PEO) (6.9 mg and 13.4 mg per mass of solution) was obtained during the preparation of precursor solution in order to slow down the crystallization process and obtain smoother film surfaces. MAI was synthesized in the Organic Electronics Lab, PbI_2 (purity of 99%)and PEO were purchased from Sigma-Aldrich.

ii. Solutions with three different MAI:SnI_2 molar ratios were prepared: 0.4:1, 0.8:1 and 1:1. The solutes were dissolved in DMF, with a total solids concentration between 35 wt% and 40 wt%. The solutions were left stirring for 12h at 100 ºC. Three different deposition techniques were performed. The first used was the well-known spin coating; the second was doctor blade and the third was drop cast. Additionally, a sequential deposition technique with MAI (in isopropanol solution) and SnI_2 (in DMF) was made. The obtained precursor film was annealed for 2h at 100ºC. SnI_2 was purchased from Sigma-Aldrich with a purity of 99%.

iii. Two different MAI:$SnBr_2$ molar ratios, 0.3:1 and 2:1, were prepared in DMF with solid concentrations in the range 30 - 35 wt%. The precursor solutions were left stirring for approximately 12h at 100 ºC. $SnBr_2$ was purchased from Sigma-Aldrich with a purity of 99%.

iv. A CsI:SnI$_2$:SnF$_2$ perovskite precursor solution with a molar ratio of 1:1:0.16 was prepared. The solute was dissolved in DMF with a concentration of 35 wt% and left stirring for 12h at 100 ºC. Again, different annealing conditions (temperature and time) of the films were used. CsI, SnI$_2$ and SnF$_2$ were purchased from Sigma-Aldrich with a purity 99.9%, 99% and 99% respectively.

The electron-accepting layer was prepared with the fullerenes C60 and/or PCBM. The C60 layer was evaporated on top of perovskite film using the PVD method (thermal evaporation). Deposition rate was between 0.5 and 1 Å/s in order to obtain a thickness of approximately 30 nm. On the other hand, PCBM was deposited by spin coating after the annealing of perovskite film. Fullerenes - C$_{60}$ and PCBM were purchased from Sigma-Aldrich and Solenne, respectively, with a purity greater than 99%.

Before the deposition of top electrodes, BPhen was deposited in some MAPbI$_3$ samples to improve the electron extraction and promote better a coverage of irregular perovskite and C60 layers. This material was also deposited by PVD. BPhen was purchased from Sigma-Aldrich with a purity of 99%.

The top electrode, composed by a thin layer of LiF (1.5 nm) and a layer of Al (approximately 100 nm), was deposited on top of EAL/BPhen by the same PVD deposition conditions. LiF was used because it reduces the work function of Al (4.3 eV) electrode, facilitating the extraction of electrons [11], [12].

3. Results and discussion

3.1 Hybrid lead-perovskites

Devices combining different MAI:PbI$_2$ molar ratios, hole (PEDOT: PSS and MoO$_3$) and electron transporting materials (PCBM, C60 and BPhen) and low work-function electrodes (Al and LiF/Al) were prepared and tested. All depositions were performed by spin coating with spinning speeds in range of (1500 - 1800 rpm) during (15 - 20s). All annealing conditions were performed at (100ºC – 150ºC) during approximately 2 h. The best result came from device 105 with

the structure ITO / PEDOT: PSS / MAPbI$_3$ / PCBM / C60 / BPhen / LiF/Al. The perovskite active layer was prepared from a solution with a molar ratio MAI:PbI$_2$ of 1.28:1. Figure 3-1 shows its current voltage characteristics recorded in the dark and under 1 Sun illumination. Table 3-1 summarizes the cell performance parameters, showing a rather low efficiency of 0.88%.

Device	Jsc (mA.cm^{-2})	Voc (V)	FF (%)	PCE (%)
ITO / PEDOT: PSS / Perovskite (1.28:1) / PCBM / C60 / BPhen / LiF/Al				
105	4.09	0.57	37.82	0.88

Table 3-1. Parameters of the best device based on lead perovskites
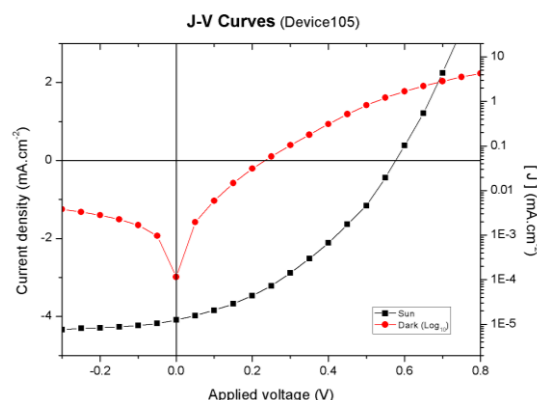

Figure 3-1. J-V curve for the best solar cell based on MAPbI$_3$ under illumination and in the dark (logarithmic scale) (Device 105)

Observing the representative J-V curve it is possible to conclude that the device exhibits a rectification in the dark, as expected for a typical diode, though it is small. We observe that under normal deposition conditions, the PCBM solution was dissolving the perovskite layer. In order to overcome this situation, PCBM solution was spin coated with the substrate already spinning to promote a fast chlorobenzene evaporation. Despite the efforts, some of the perovskite layer was dissolved and removed from the substrate. We also concluded that we need to use a small excess of MAI, with respect to PbI$_2$ in order to achieve the complete dissolution of the lead iodide in DMF.

In view of the concerns about the perovskite stability when exposed to normal atmosphere, we recorded the absorption spectrum of a film of MAPbI$_3$ right after its

removal from the glove box and after 5 min exposure to air. From the obtained spectra, shown in Figure 3.1-2 we conclude that there is a decrease of film absorption, thereby indicating its degradation over the time.
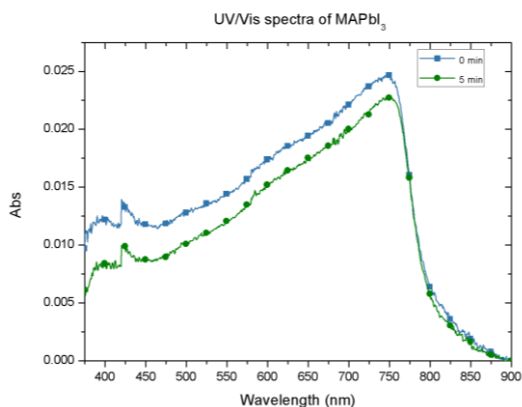

Figure 3-2. UV/Vis spectra of a MAPbI$_3$ perovskite film (prepared by spin coating on a quartz substrate from a 1.28:1 solution)

The optical gap ΔE_{Gap}, determined from the absorption onset, is 1.53 eV remaining almost unaltered after 5 min. This energy gap value is in agreement with the reported value for this perovskite type [13].

3.2 Hybrid tin-perovskites

Devices with two different perovskites MASnI$_3$ and MASnIBr$_2$ were fabricated and tested. Three different deposition methods were used in these thin films fabrication; spin coating, doctor blade and drop cast. All the annealing process occurred at (100 - 115ºC) during approximately 2h. A sequential deposition of MAI and then SnI$_2$ was tested but did not improve the PCE value. Among all the tested tin-based devices, the best performing one (device 115) was based on MASnIBr$_2$, having the structure: ITO / PEDOT: PSS / MASnIBr$_2$ / C60 / BPhen / LiF/Al, where the perovskite was prepared from a solution with MAI:SnBr$_2$ molar ratio of 2:1. The corresponding parameters are shown in Table 3-2, and current density-voltage curves are presented in Figure 3-3.

Device	Jsc (mA.cm^{-2})	Voc (V)	FF (%)	PCE (%)
ITO / PEDOT: PSS / Perovskite (2:1) / C60 / BPhen / LiF/Al				
115	0.33	0.24	25.86	2.00 x 10^{-2}

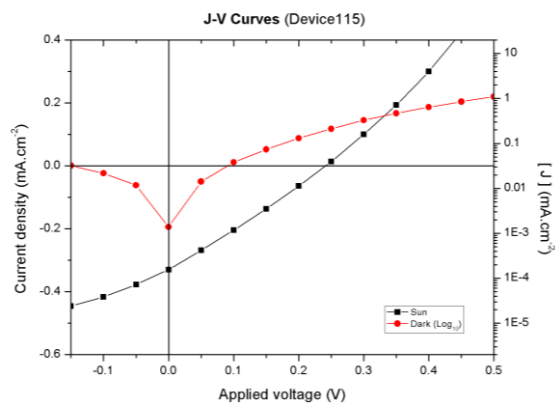*Table 3-2. Parameters of the best device based on MASnIBr$_2$ perovskite*

Figure 3-3. J-V curve for the best solar cell based on MASnIBr2 under illumination and in the dark (logarithmic scale) (Device 115)

Observing figure 3-3, we conclude that dark the J-V curve does not show significant rectification. Once again, at variance with literature reports, we could not obtain smooth perovskite surfaces.

3.3 Inorganic cesium-perovskites

A fully inorganic perovskite, consisting on CsSnI$_3$ doped with SnF$_2$, was also tested. Despite the many efforts, keeping always the same solution composition, deposition process and annealing conditions, but for different devices structures we did not obtain devices showing meaningful efficiency.

4. Conclusions

In this work we prepared and tested more than one hundred photovoltaic cells with four different types of perovskites; MAPbI$_3$; MASnI$_3$; MASnIBr$_3$; CsSnI$_3$+SnF$_2$. All solutions were prepared and deposited in a nitrogen-filled glove box. For each perovskite various preparation conditions and device structures were tested. All the obtained results remained well below the reported values in literature. The best performing device was based on the MAPbI$_3$ perovskite, showing the following parameters: J$_{sc}$ of 4.09 mA.cm^{-2}, V$_{oc}$ of 0.57 V, FF of 37.82 % and PCE of 0.88%. In December 2015, Grätzel et al. [14] obtained the highest PCE value in the world for these photovoltaic cells with MAPbI$_3$ perovskite films. The main obstacle we faced during this project was the preparation of clear solutions and good quality films. The poor crystallization was observed through a

sudden change in perovskite color from yellow to dark brown in a manner of seconds. Despite these poor results, this work provided a research direction mainly focused on the optimization of the molar ratio between (MAI) and the inorganic perovskite component, as we concluded that an excess of MAI is needed to increase the dissolution of lead and tin salts in DMF.

Once the previous goal is achieved, there remain the tasks related to the optimization of the photovoltaic cell structure, namely in terms of right thickness of the electron-donor layer once it greatly influences PCE values. We believe that, combining these approaches with novel heterojunction surface morphologies between electron-donor / acceptor materials, the overall parameters will increase leading to higher PCE results.

References

[1]   G. Crabtree, E. Kocs, and T. Aláan, "Energy, society and science: The fifty-year scenario," *Futures*, vol. 58, pp. 53–65, Apr. 2014.

[2]   T. C. Sum and N. Mathews, "Advancements in perovskite solar cells: photophysics behind the photovoltaics," *Energy Environ. Sci.*, vol. 7, no. 8, pp. 2518–2534, May 2014.

[3]   L. D. P. Lewis M. Fraas, *Solar Cells and Their Applications.* Wiley, 2010.

[4]   N.-G. Park, "Perovskite solar cells: an emerging photovoltaic technology," *Mater. Today*, vol. 18, no. 2, pp. 65–72, Mar. 2015.

[5]   J. M. T. Pereira, "Semicondutores," in *Fundamentos de Electrónica*, Lisboa, 2010, pp. 1–68.

[6]   A. M. Gheidari, E. A. Soleimani, M. Mansorhoseini, S. Mohajerzadeh, N. Madani, and W.-S. Kolahi, "Structural properties of indium tin oxide thin films prepared for application in solar cells," *Mater. Res. Bull.*, vol. 40, no. 8, pp. 1303–1307, 2005.

[7]   M. S. Farhan, E. Zalnezhad, A. R. Bushroa, and A. A. D. Sarhan, "Electrical and optical properties of indium-tin oxide (ITO) films by ion-assisted deposition (IAD) at room temperature," *Int. J. Precis. Eng. Manuf.*, vol. 14, no. 8, pp. 1465–1469, 2013.

[8]   A. Uygun, O. Turkoglu, S. Sen, E. Ersoy, A. G. Yavuz, and G. G. Batir, "The electrical conductivity properties of polythiophene/TiO2 nanocomposites prepared in the presence of surfactants," *Curr. Appl. Phys.*, vol. 9, no. 4, pp. 866–871, 2009.

[9]   Heraues, "Organic and 3rd generation Solar Cells," 2015. [Online]. Available: http://www.heraeus-clevios.com/en/applications/solarcells/organic-solar-cells.aspx. [Accessed: 18-Jun-2015].

[10]   S. Calnan, "Applications of Oxide Coatings in Photovoltaic Devices," *Coatings*, vol. 4, no. 1, pp. 162–202, Mar. 2014.

[11]   H.-L. Cheng and K.-F. Lin, "Enhancing emission of poly(p-phenylenevinylene) by sandwiching an energy transferable layer," *J. Mater. Chem.*, vol. 12, no. 8, pp. 2270–2274, Jul. 2002.

[12]   C. J. Brabec, S. E. Shaheen, C. Winder, N. S. Sariciftci, and P. Denk, "Effect of LiF/metal electrodes on the performance of plastic solar cells," *Appl. Phys. Lett.*, vol. 80, no. 7, pp. 1288–1290, 2002.

[13]   P. Gao, M. Grätzel, and M. K. Nazeeruddin, "Organohalide lead perovskites for photovoltaic applications," *Energy Environ. Sci.*, vol. 7, no. 8, p. 2448, Jun. 2014.

[14]   M. Grätzel, "EPFL Achieves 21% Efficiency for Perovskites," no. December. DYESOL LTD, p. 1, 2015.